PAPER 6

Multi-temporal JERS SAR data in boreal forest biomass mapping

In: Remote Sensing of Environment 2005.
Vol. 97, pp. 263–275.
Reprinted with permission from the publisher.

Reprinted from Remote Sensing of Environment, Vol. 97, Rauste, Y., Multi-temporal JERS SAR data in boreal forest biomass mapping, p. 263–275, Copyright (2005), with permission from Elsevier.

Available online at www.sciencedirect.com
SCIENCE DIRECT
Remote Sensing of Environment 97 (2005) 263 – 275
Remote Sensing of Environment
www.elsevier.com/locate/rse

Multi-temporal JERS SAR data in boreal forest biomass mapping

Yrjo Rauste

VTT Technical Research Centre of Finland, Finland

Received 28 March 2003; received in revised form 29 March 2005; accepted 19 May 2005

Abstract

Multi-temporal JERS SAR data were studied for forest biomass mapping. The study site was located in South-eastern Finland in Ruokolahti. Pre-processing of JERS SAR data included ortho-rectification and radiometric normalization of topographic effects.

In single-date regression analysis between backscatter amplitude and stem volume, summer scenes from July to October produced correlation coefficients (r) between 0.63 and 0.81. Backscatter level and the slope of the (linear) regression line were stable from scene to scene. Winter scenes acquired in very cold and dry winter conditions had a very low correlation. One winter scene acquired in conditions where snow is not completely frozen produced a correlation coefficient similar to summer scenes.

Multivariate regression analysis with a 6-date JERS SAR dataset produced correlation coefficient of 0.85. A combined JERS–optical regression analysis improved the correlation coefficient to 0.89 and also alleviated the saturation, which affects both SAR and optical data.

The stability of the regression results in summer scenes suggests that a simple constant model could be used in wide-area forest biomass mapping if accuracy requirements are low and if biomass estimates are aggregated to large areal units.
© 2005 Elsevier Inc. All rights reserved.

Keywords: Remote sensing; Biomass; Microwave; Boreal forest

1. Introduction

Standing forest biomass forms an essential part of active carbon pool participating in the global carbon cycle. Mapping the amount and geographic distribution of forest biomass – and its change with time – is important for understanding the development of the carbon cycle. Main part of forest biomass in boreal forests is in tree stems, which can be used as raw material in wood and pulp industry. Information on the spatial distribution of forest biomass is therefore important for forest industry and sustainable forestry.

In the GRFM (Global Rain Forest Mapping) project, several continental SAR mosaics were produced for tropical areas. In a follow-on project GBFM (Global Boreal Forest Mapping), similar mosaics are being produced for the whole boreal forest belt of the world (Rosenqvist et al., 2000). These mosaics can serve as a starting point and important input dataset when global forest biomass evaluations are made for carbon cycle studies and other environmental applications. In the context of the GBFM project, a Northern Europe science node was organised by Metria Miljoanalys (Jonsson, 2002) as a "regional exploratory addition to the GBFM programme".

Most of the forest biomass in boreal forests is in tree stems. Since large datasets on biomass measurements in boreal forests are difficult to obtain, stem volume data from forest inventory data bases are widely used instead of forest biomass. As an approximation, forest stem volume (m^3/ha) in boreal forests can be converted into dry biomass (tons/ha) by multiplying the stem volume estimate by 0.6 (Häme et al., 1992).

Active microwave sensors from 10-GHz X-band (e.g., Beaudoin et al., 1992; Le Toan et al., 1992) to 28- to 80-MHz VHF SAR (e.g., Israelsson et al., 1997) have been studied for forest biomass mapping. X-band has the lowest dynamic range and sensitivity to forest biomass (Le Toan et al., 1991). The three-band (C, L, and P) polarimetric AIRSAR sensor has been used in many forest biomass

E-mail address: Yrjo.Rauste@vtt.fi.

0034-4257/$ - see front matter © 2005 Elsevier Inc. All rights reserved.
doi:10.1016/j.rse.2005.05.002

studies (e.g., Green, 1998; Kasischke et al., 1991, 1995; Moghaddam et al., 1994; Ranson & Sun, 1997). The strongest correlation between SAR backscatter and forest biomass has been reported in P-band and the weakest in C-band (e.g., Beaudoin et al., 1992; Dobson et al., 1992; Israelsson et al., 1992; Rauste et al., 1992; Skriver & Gudmandsen, 1992). A spaceborne P-band SAR will not be available in the foreseeable future even though it has been proposed (e.g., Rignot et al., 1995). Despite the very strong backscatter–biomass relation in VHF SAR (Melon et al., 2001, report even a 0.99 correlation), a spaceborne VHF SAR is not practical. Studies using dual-frequency (C- and L-bands) polarimetric SIR-C data (e.g., Dobson et al., 1995; Harrell et al., 1997) point out the importance of L-band data in coniferous forest biomass mapping.

The correlation between forest biomass and the C-band backscatter measured by the ERS-1 and ERS-2 SAR sensors has been reported to be low in tropical forests (e.g., Luckman et al., 1997) and oil palm and rubber plantations (Rosenqvist, 1996). Kasischke et al. (1994) describe the C-band dynamic range due to biomass variation as low in young loblolly pine forests. In boreal forests, the biomass vs. C-band backscatter correlation depends heavily on the soil moisture conditions (Pulliainen et al., 1994, 1997; Wang et al., 1994). Pulliainen et al. (1996) have used a highly multi-temporal ERS dataset and a semiempirical backscatter model for boreal forest biomass estimation. A correlation coefficient (r) of 0.66 was obtained in a test site where the stem volume ranged from 0 to 300 m^3/ha. Since the method includes per-scene soil and vegetation moisture variables (and biomass reference data), its use in wide-area biomass mapping may be difficult.

Repeat-pass interferometry with C-band ERS data has been studied for forest biomass mapping (e.g., Fransson et al., 2001; Luckman et al., 2000). Luckman et al. (2000) obtained a coefficient of determination (R^2) of 0.805 between ERS-1/2 (1-day difference) tandem coherence and the logarithm of forest biomass in regenerating tropical forests (biomass mainly between 0 and 100 tons/ha). Fransson et al. (2001) studied 5 ERS-1/2 interferometric pairs of a test site where stem volume ranges from 0 to 300 m^3/ha. The highest (adjusted) coefficient of determination (R_A^2) between stem volume and ERS coherence was 0.87 while the lowest was 0.06. In a more recent study, Pulliainen et al. (2003) used 14 ERS-1/2 interferometric pairs (1-day difference in scene acquisition) in a Finnish site (stem volume 0...539 m^3/ha, mean stem volume 174 m^3/ha). The correlation coefficient (r) between coherence and stem volume varied mainly between 0.46 and 0.87 while one pair (during snow melting period) had an r value of 0.07. These last two examples suggest, as Pulliainen et al. (2003) note, that the repeat-pass interferometry in forest biomass mapping is influenced by weather conditions.

Even though L-band backscatter is stronger correlated with forest biomass, a limiting factor is the saturation of the backscatter–biomass relationship at some biomass level (Imhoff, 1993). Based on a dataset combined from three test sites (Hawaii/USA: broad-leaved, North Carolina/USA: pine forests, and France: pine forests), Imhoff (1995) reports the L-band saturation level at 40 tons/ha of dry biomass. Luckman et al. (1998) found a saturation of 60 tons/ha in a Brazilian test site. In boreal forests, the 40 tons/ha limit corresponds to a forest stem volume of approximately 70 m^3/ha. Israelsson et al. (1995) found the saturation level of 100 to 150 m^3/ha in a boreal test site in Sweden and Fransson and Israelsson (1999) obtained a saturation level of 143 m^3/ha. Rauste et al. (1994) found an L-band saturation level of about 120 m^3/ha in a coniferous forest site in Germany. Kurvonen et al. (1999) report a saturation level of 225 m^3/ha in two JERS SAR scenes. Toshio et al. (1995) obtained a correlation coefficient (r) of 0.75 between forest stem volume and JERS SAR amplitude in a test site in Japan where the forest stem volume goes up to 900 m^3/ha. So the saturation level may depend on the tree species and forest types as well as the ground surface type. In addition to tree species, the L-band backscatter vs. biomass relationship also depends on forest management practices. Kuplich et al. (2000) found a strong L-band vs. biomass correlation ($r=0.77$) in a Brazilian test site (re-growth after a clear cut) while the correlation was weak in a Cameronian test site (selective logging). Paloscia et al. (1999) report an r^2 value (between the logarithm of woody biomass and logarithm of backscatter power) of 0.77 using a few forested areas in a JERS-1 SAR dataset in Italy. Kellndorfer et al. (2001) report an adjusted R_A^2 values of 0.72 and 0.56 (between the logarithm of biomass and logarithm of backscatter power) for two JERS SAR scenes in Michigan in a stand-wise dataset consisting of 39 pine stands. Smith et al. (1998) report R^2 values of 0.27 and 0.30 for two summer-time JERS SAR scenes (uncalibrated) in a Finnish study site in stands with stem volumes 0...150 m^3/ha.

Fransson and Israelsson (1999) and Harrell et al. (1995) have published regression models between L-band backscatter and forest biomass (see later chapter comparison of new regression models and existing models).

Dobson et al. (1991) observed that a rain shower had the strongest effect (in a C-, L-, and P-band dataset) on C-band data and the weakest effect on the P-band data. The stability of the relation between polarimetric P-band data and forest biomass through the growing season was also confirmed by Rauste (1993). Chipman et al. (2000) observed (in a C- and L-band dataset) that the L-band is likely to be more temporally stable than the C-band. Since boreal forest environment – with low temperatures and seasonal snow cover – has widely variable physical attributes for microwave scattering, the seasonal variations in L-band SAR data can be expected to be pronounced in boreal forests (e.g., Pulliainen et al., 1999).

The literature has documented the relationship of L-band backscatter and forest biomass. Seasonal effects in this relationship have also been observed. These observations are rather occasional. No systematic effort to

exploit these seasonal effects in L-band biomass mapping has been documented in literature. The objectives of the study were:

1. To study seasonal variation in L-band SAR data and the potential of L-band SAR data acquired in various seasons in mapping the biomass of boreal forest;
2. To study the potential of combining L-band SAR data and optical satellite data in boreal forest biomass mapping.

2. Materials and methods

2.1. Ground data

The study site (centre 61°31′N, 28°46′E) was located in Puumala and Ruokolahti in South-eastern Finland. The dominant soil type in the site is glacial drift. The most common tree species was pine (*Pinus sylvestris*). Other common species were spruce (*Picea abies*) and birch (*Betula betula*).

Ground data came from two sources: (1) stand-wise forest inventory data from Stora Enso Ltd., and (2) a set of point-wise measurements made by the Finnish Forest Research Institute.

The stand-wise forest inventory data included one forest stem volume for the whole stand. Since this dataset was compiled for practical forest management purposes, its accuracy is not perfect. The forest inventory was made in 1997. The stand-wise forest inventory data were turned to image format and resampled to 25 m pixels as used in the ortho-rectification of the SAR data. One erosion step (pixels whose all neighbouring pixels are not of the same stand as the pixel itself rejected) was done to the ground data image. Stands smaller than 2 ha (32 pixels) were excluded. The forest inventory dataset finally included 206 stands covering 845 ha. The average stem volume within these 206 stands was 102 m^3/ha (lowest 0 m^3/ha, highest 364 m^3/ha, standard deviation 79 m^3/ha).

The point-wise (plot) ground data covered a 1-km-by-1-km area with a regular grid of points at a distance of 50 m (20 lines by 20 columns). The average stem volume within the point-wise ground dataset was 104 m^3/ha (lowest 0 m^3/ha, highest 355 m^3/ha, standard deviation 68 m^3/ha). Total stem volume measurement data were used as an independent test data for JERS-derived biomass estimates.

A digital elevation model (DEM) was used for ortho-rectification of JERS SAR data. The DEM was produced with contour-line data from 1:20,000 topographic maps. The pixel spacing in the DEM was 25 m and the vertical accuracy about 2 m. The DEM covered an area of 38.15 km (in northing) by 50.85 km (in easting).

2.2. SAR data

The conceptual model of seasonal changes included 5 seasonal configurations based on meteorological and physical conditions controlling overall backscattering and the phenological state of trees:

1. the peak bio-chemical activity during the first half of the growing season (G1),
2. the second half of the growing season before the drop of the leaves of deciduous trees (G2),
3. leaves-off period before the first snow (G3),
4. cold winter conditions (WD), and
5. wet winter conditions (WW).

The aim in image selection was to obtain at least one scene from all seasons defined above. Only those descending-orbit scenes were considered that were acquired on the same track as the first scene (20.02.1993) of the dataset. Some scenes that were listed in JERS SAR catalogues were not of high enough quality for SAR processors. Table 1 shows the scenes that were available for analysis. The first growing season configuration (G1) remained missing due to quality problems of raw SAR data. The meteorological data in Table 1 are from the airport of Lappeenranta 60 km from the study site. Temperatures (min and max) are for the image acquisition day. Precipitation data are for the acquisition day (column Day) and the day preceding the acquisition day (column Prev). The form of precipitation has been snow on 20.2.1993 and 14.3.1998 and water on 20.7.1995, 2.9.1995, and 16.10.1995. On 25.1.1995, the precipitation may have been either water or snow or – most likely – wet snow. The summer and autumn scenes (20.7.1995, 2.9.1995, and 16.10.1995) are all from reason-

Table 1
JERS SAR scenes used and the meteorological conditions (in Lappeenranta airport)

Acquired	Temperature (°C)		Precipitation (mm)		Frost days	Conf	Processor
	Max	Min	Day	Prev			
20.02.1993	−5.8	−11.2	2.4	7.7	4	WD	ESA
25.01.1995	0.2	−2.1	1.4	9.7		WW	NASDA/ERS-DPS/434
20.07.1995	20.4	12.0	0.2	1.6		G2	NASDA/ERS-DPS/434
02.09.1995	17.0	8.0	0.1	2.4		G2	NASDA/ERS-DPS/434
16.10.1995	8.6	0.6	1.5	0.1		G3	NASDA/ERS-DPS/434
14.03.1998	−9.0	−13.6	0.7	2.8	13	WD	NASDA/Sigma-SAR

ably dry conditions. Precipitation of only 0.2... 1.5 mm suggests that the rain has been light, low intensity showers, where the water evaporates from leaves and other canopy components in a matter of an hour or less. Because there has been some precipitation, trees and other plants have not been plagued by drought. Column Frost days gives the number of days during which the maximum temperature has been below 0 °C before the image acquisition day. Column Conf gives the classification of the meteorological conditions to the seasons listed above. Column Processor gives the SAR processor used to generate the SAR image product.

Most of the SAR scenes were within 2 years from the forest inventory (summer 1997). Since the yearly growth in the climatic conditions of the study site is only a few percent, the data can be considered to be from the same time as the SAR data.

A Landsat TM scene acquired on 29 August 1997 was used to study SAR-optical synergy.

2.3. Pre-processing of SAR data

The SAR data that stemmed from 3 different SAR processors were not calibrated to the same standard. The older NASDA processor (ERS-DPS, version 434) was chosen as a reference and the remaining two scenes were scaled to that system. The first scene (acquired on 20.2.1993, no calibration data were supplied with the data) was approximately calibrated. Two sample areas were chosen in mature forest areas and in water areas. Image data ratio (in amplitude) was computed between the average of the 4 scenes of 1995 and the scene of 20.2.1993. An average between the water and forest ratio was calculated. The scene of 20.2.1993 was scaled by this factor to approximately match the scenes of 1995. The scene acquired on 14.3.1998 was scaled (the amplitude values of this scene were multiplied by 0.139) to take into account the difference in calibration factors of the older NASDA processor (68.2 dB, Shimada, 1996, 2001) and the Sigma-SAR processor (85.34 dB, Shimada & Isoguchi, 2002).

The JERS SAR scenes were ortho-rectified to 25-m pixel spacing. The rectification made use of tie points between scenes, ground control points (GCPs) between scenes and topographic maps, and block adjustment by the least squares method (see De Grandi et al., 2000). Affine (6 parameter) geometric model was used in the block adjustment. The tie point RMSE (Residual Mean Square Error) was 19 m in northing and 12 m in easting. The GCP RMSE was 24 m in northing and 22 m in easting.

JERS SAR data were radiometrically normalized in connection with ortho-rectification:

$$\mathrm{DN_{out}} = \mathrm{DN_{in}}{*}\mathrm{sqrt}\left(\tan\left(\theta_R^{\mathrm{local}}\right)/\tan(\theta_o)\right) \quad (1)$$

where $\mathrm{DN_{out}}$ = normalized pixel amplitude, $\mathrm{DN_{in}}$ = input pixel amplitude, $\theta_R^{\mathrm{local}}$ = the local incidence angle in the vertical cross-track plane, θ_o = the nominal incidence angle of the sensor (38°).

This normalization gives a constant response (with respect to incidence angle) for targets whose backscattering coefficient γ° (not σ^{O}) is uniform with respect to incidence angle.

An adaptation of median and average filtering (5-out-of-9 filtering) was used in speckle reduction of JERS SAR scenes. Pixel values in each 3-by-3 window are sorted. The highest 2 values and the lowest 2 values are excluded. A weighted average is computed of the remaining 5 pixels. The weighting function is Gaussian with standard deviation of half a pixel. This filtering was used when producing pixel-wise stem volume maps, not in connection with regression analysis.

2.4. Regression analysis

Regression analysis is an appropriate statistical technique to study the relationship between continuous variables such as forest biomass and radar backscatter. Regression analysis (both single-variable and multivariate regression analysis) was used in stem volume estimation. Stand-wise forest inventory data were used as training data to derive regression models between stem volume (the dependent variable) and various sets of JERS SAR and Landsat TM data as independent variables. The earth observation data were averaged for the 206 stands using a stand mask image to obtain the value of the independent variable(s). The JERS SAR amplitude data were squared before averaging and a square root was taken after the averaging. The stem volume of the stand (just one figure per stand) was used as the value of the dependent variable.

Past studies (e.g., Rauste et al., 1994) have shown that a fairly linear relationship (at least for low biomass levels) can be expected between forest stem volume and radar backscatter amplitude. Since the variable to estimate was stem volume, not the logarithm of stem volume, any non-linear transformations could only be applied to radar backscatter data. The JERS SAR data were supplied by NASDA in the form of backscatter amplitudes. Because amplitude is a widely used form of SAR data distribution, JERS SAR data were input in regression analysis as amplitude values. The form of the regression function in single-date regression analysis was:

$$V = A{*}\mathrm{DN_{JERS}} + B \quad (2)$$

where V = stem volume ($\mathrm{m^3/ha}$), $\mathrm{DN_{JERS}}$ = JERS SAR amplitude scaled as in the scenes used in this study, i.e., $\sigma^{\circ} = 10{*}\log_{10}(\mathrm{DN_{JERS*}}\cdot\mathrm{DN_{JERS}}) - 68.2$ dB, A = slope of the regression model, B = intercept of the regression model.

Multivariate regression analysis was used to study the increased potential of multi-temporal L-band SAR data in forest biomass mapping.

The relationship between forest stem volume (or biomass) and L-band radar backscatter saturates somewhere

between 100 m^3/ha and 200 m^3/ha. For this reason, regression analyses were made in a series of steps leaving a part of the stem volume range out. The reference case included all stands (with stem volume range 0...360 m^3/ha). The first set of cases included the upper end of the stem volume range present in the study site. The lower limit of the stem volume range was increased in steps (50, 100, 150 and 200 m^3/ha). The second set of cases included the lower part of stem volume range. In this set of cases, the upper limit of the stem volume range was decreased in steps (300, 250, 200, 150, 100, and 50 m^3/ha). Because the number of observations varied from 19 to 206, an adjusted R^2 was also computed in addition to the usual coefficient of determination:

$$R_A^2 = R^2 - \left(1 - R^2\right)p/(n - p + 1) \quad (3)$$

where R_A^2=adjusted R^2, R^2=coefficient of determination, n=number of observations, and p=number of predictor variables (6 SAR scenes).

The accuracy of JERS-SAR-based stem volume estimate was measured by root-mean-square error:

$$\mathrm{RMSE} = \mathrm{sqrt}\left(\Sigma\left(V_g - V_J\right)^2/(n-2)\right) \quad (4)$$

where RMSE=root-mean-square error, V_g=stem volume in ground data, V_J=stem volume in JERS-based estimate, and n=number of observations.

3. Results and discussion

3.1. Single-date regression models

Table 2 shows regression results for each of the JERS SAR scenes against forest stem volume. Column Vol-Rg shows the range of stem volume of the stands that were included in the analyses. Column n shows the number of stands. The variation by one stand is due to a slightly varying coverage of the scenes. Columns A and B show the coefficients of a linear regression model (Eq. (2)) between JERS SAR amplitude and stem volume. Column r in Table 2 shows the correlation coefficient between SAR amplitude and stem volume. Coefficient of determination is R^2. The scene identifiers in Table 2 are of the form:

CYYMMM

where C=designation of the seasonal configuration: dry for the winter/dry scenes, wet for the winter/wet scene, and S for the summer scenes, YYMMM=acquisition year (YY) and month (MMM). The full acquisition date is shown in Table 1.

Table 2
Regression results between forest stem volume and single-date JERS SAR data

Scene	Vol-Rg	n	A	B	r	R^2
S95Jul	0–360	205	0.60	−562	0.81	0.66
S95Sep	0–360	205	0.72	−743	0.70	0.49
S95Oct	0–360	206	0.87	−894	0.63	0.40
Dry93Feb	0–360	206	3.22	−3239	0.40	0.16
Wet95Jan	0–360	206	0.71	−560	0.78	0.61
Dry98Mar	0–360	206	−30.33	26896	−0.05	0.00
Summer	0–360	616	0.71	−713	0.71	0.50
Summer	10–360	529	0.65	−634	0.73	0.53

The lines titled Summer at the end of Table 2 combine all observations of scenes S95Jul, S95Sep, and S95Oct into a single dataset. The 616 observations in the summer dataset are not completely independent because the stands cover the same area on the ground, and therefore, three observations have the same value of dependent variable. The observations of the SAR backscatter are independent because the speckle and other noise sources are independent from scene to scene.

The regression model of the combined summer dataset can be written:

$$V = 0.65\ \mathrm{sqrt}\left(10^{\left(\left(\sigma^O + 68.2\right)/10\right)}\right) - 634 \quad (5)$$

where σ^O=backscattering coefficient in dB and V=stem volume in m^3/ha. The corresponding model for forest biomass (dry) is:

$$B = 0.39\ \mathrm{sqrt}\left(10^{\left(\left(\sigma^O + 68.2\right)/10\right)}\right) - 380 \quad (6)$$

where B=dry biomass in tons/ha.

Fig. 1 shows the stand average data and regression lines separately for winter and summer scenes. The correlation between stem volume and JERS SAR data is very weak in winter scenes acquired in cold, dry conditions (scenes Dry93Feb and Dry98Mar in Fig. 1). Correlation coefficients are low (0.4 and −0.05). There is a more pronounced relationship between the JERS SAR data and stem volume in summer scenes. Correlation coefficients range from 0.63 to 0.81. The form of the relationship (regression lines in Fig. 1 and A and B coefficients in Table 2) is similar from scene to scene. No significant difference can be seen between the scenes acquired in leaves-on conditions (S95Jul and S95Sep) and the scene acquired in leaves-off conditions (S95Oct). The slope of the regression line is slightly lower in the late-autumn scene and its correlation coefficient is slightly lower than that of the July–September scenes, though. All three estimator lines (S95Jul, S95Sep and S95Oct) are within 60 m^3/ha from each other over the whole range from 0 to 200 m^3/ha. This suggests that a linear model with constant coefficients can be used to produce an estimate of forest stem volume when using L-band SAR data acquired in reasonably dry summer conditions, especially if accuracy requirements are not high.

The scene Wet95Jan forms an exception in the set of winter scenes. Correlation coefficient (0.78) is as high as in

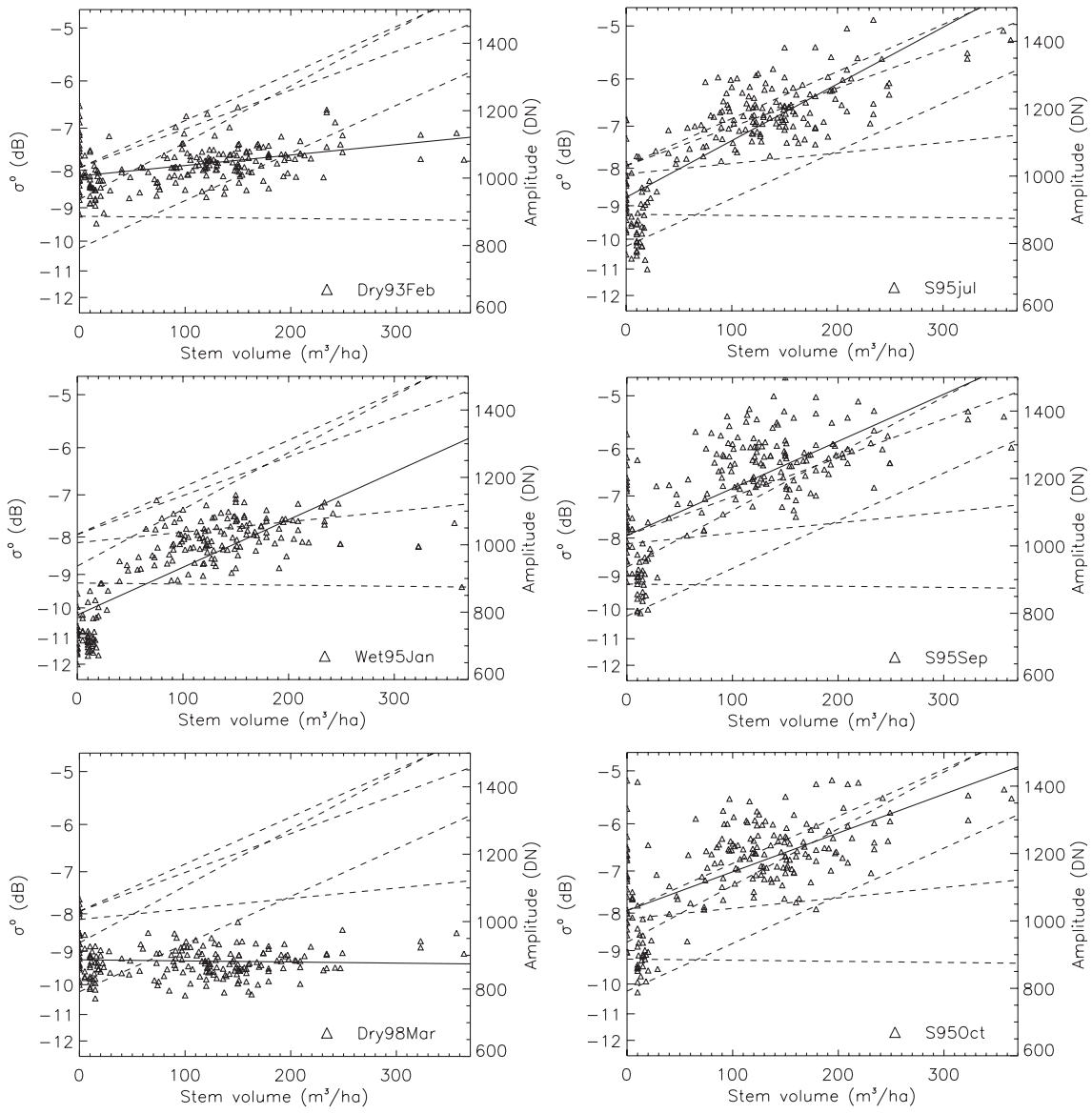

Fig. 1. Regression diagrams between forest stem volume and JERS SAR data for winter (left) and summer (right) scenes. The solid line shows the regression line computed from the observation data in the diagram. The dashed lines are the regression lines from the other 5 scenes.

a typical summer scene. The slope of the regression line is also very similar to the summer scenes, but the overall backscattering level is lower in this winter scene, which was acquired in conditions with a moist layer of new snow on top of older snow layers. In addition to high stem volume vs. backscatter correlation, the scene Wet95Jan discriminates well between clear-cut areas and forest.

Fig. 2 shows one mechanism that can explain the separability of clear-cut areas in scene Wet95Jan. In normal dry winter conditions, the backscatter from the snow pack (with various ice crust layers and other ice objects inside) and from the underlying soil surface (in clear-cut areas) is about as high as the backscatter from various components of forest canopy. If there is a layer of new snow (or snow with a high moisture content in general), the backscatter from the snow pack and underlying soil is absorbed in the clear-cut areas while the canopy backscatter in forested areas remains about the same as in dry winter conditions. This generates a difference between clear-cut areas and forest in the scene in wet winter conditions. The lower the stem volume, the closer a stand is to the clear-cut case, which creates a positive correlation between stem volume and backscatter.

3.2. Comparison of new regression models and existing models

Harrell et al. (1995) found a regression model between total biomass and JERS-1 SAR backscatter:

$$y = 2.555\log(x) - 9.644 \quad (7)$$

where x = total biomass (kg/m^2) and y = backscattering coefficient (dB). The model was derived in an Alaskan test

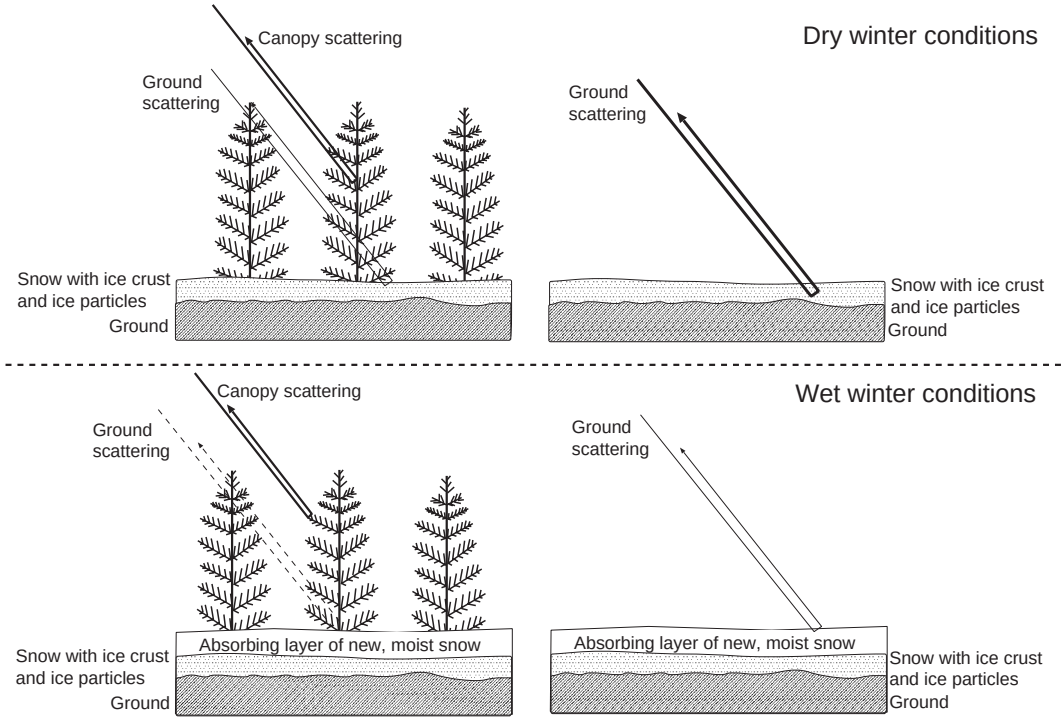

Fig. 2. Forest and clear-cut backscatter (schematically) in dry and wet winter conditions.

site (11 stands) with the total biomass ranging from 1 to 6 kg/m^2 (10 to 60 tons/ha). The JERS SAR data were acquired in July–August 1992.

Fransson and Israelsson (1999) found a regression model between stem volume and JERS-1 SAR backscatter:

$$V = 786 + 79\sigma^O \tag{8}$$

where σ^O=backscattering coefficient (dB) and V=stem volume (m^3/ha). The model was derived in a Swedish study site close to Umeå (37 stands) with the stem volume ranging from 0 to 300 m^3/ha. The JERS SAR data were acquired in June 1992.

Published regression models from literature can be directly compared to regression models derived using calibrated data. Fig. 3 shows the JERS SAR summer data from the Ruokolahti study site. The continuous line is the regression line corresponding to these points. Data for a Finnish Boreal forest study site by Pulliainen et al. (1999) has also been included in Fig. 3. These data were averaged over a JERS image (23 May 1993) for 6 stem volume classes based on a forest map by the Finnish Forest Research Institute. The curvilinear dotted line that ends at 100 m^3/ha is from Harrell et al. (1995). The biomass values have been converted to stem volume by the formula (Häme et al., 1992):

$$V = B/0.6 \tag{9}$$

where V=stem volume (m^3/ha) and B=dry biomass (tons/ha). The JERS SAR data of Harrell et al. (1995) were acquired in July–August 1992. The test site of Harrell et al. (1995) was in Interior Alaska with a fairly low biomass level. The almost linear dashed line in Fig. 3 is from Fransson and Israelsson (1999). This model is based on JERS SAR data acquired on 17 June 1992. The slight curvature of the Fransson–Israelsson model is due to the fact that this model was determined as a linear regression between the logarithm of the backscattering coefficient (σ^O in dB) and stem volume. The Ruokolahti model was determined as a linear regression between the square root of the backscattering coefficient (amplitude) and the stem volume.

The Harrel et al. model in Fig. 3 fits the data from the Ruokolahti site fairly well. The form of the model seems

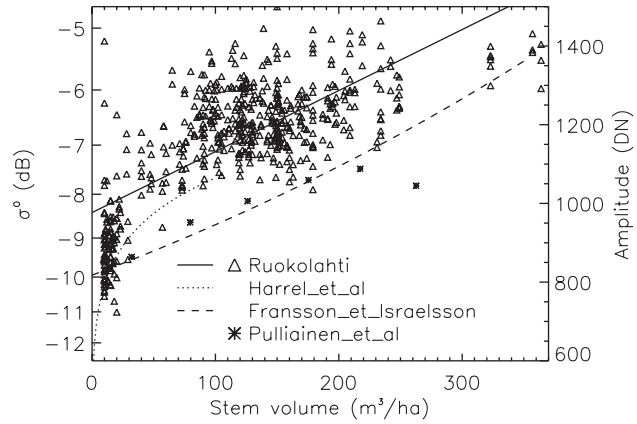

Fig. 3. Summer-time JERS data with the models of Harrell et al. (1995) and Fransson and Israelsson (1999). The observation data of Pulliainen et al. (1999) is also shown. The solid line is the regression model corresponding to line "Summer, 10–360" in Table 2.

appropriate in the narrow stem volume range. Young stands (stem volume less than 30 m^3/ha) are not very well in line with this model. This may be due to soil effects (outcrops and stones in Ruokolahti site).

Fransson and Israelsson (1999) model (dashed line in Fig. 3) and the data by Pulliainen et al. (1999) are about 1.3 dB lower than the Ruokolahti data. The difference is within the limits of calibration accuracy. Shimada (1996) reports a standard deviation of 1.86 dB for the JERS SAR calibration factor. In addition, the Umeå study site used by Fransson and Israelsson (1999) is situated on the West coast of Gulf of Botnia. In this type of area, a descending-orbit JERS SAR scene can include sea area in the near-range part of the scene. Shimada (2001) points out that the NASDA-supplied calibration factor is not valid in this situation because the AGC (Automatic Gain Control), which measures the average backscatter level from the near-range 18 km zone, causes the raw data to saturate. This in turn leads to a reduced backscatter level in the processed scene. The JERS SAR data of 21 May 1994 in Fransson and Israelsson (1999) fit well the Ruokolahti data. The numerical values for the 21 May 1994 regression line were not included in Fransson and Israelsson (1999).

The reason why the backscatter data of Pulliainen et al. (1999) are lower than in the current study may be a higher soil moisture in spring (May) after snow melt. The attempt to obtain JERS data of late spring or early summer failed in the current study.

The regression models derived in this study are valid for stands where the species composition is similar to that in the study site, typically pine or spruce dominated mixed forest. If these models are applied to sites where trees of very different canopy structure (e.g., multi-stem deciduous trees like rowan) are common, the models perform worse. Coniferous and conifer-dominated mixed forests dominate in the boreal forest zone.

3.3. Multi-date regression models

Table 3 shows the results of two sets of multivariate regression analyses. Column R^2 gives the coefficient of determination. Column r gives the correlation coefficient between the estimated stem volume and the ground data (for comparison with the data of Table 2). Column. R_A^2 gives the adjusted R^2, which takes into account the variation in the number of observations (Eq. (3)). The significance columns give the result of the t test that tests the significance of the independent variable in the regression function.

In the first set of cases, the correlation coefficient decreases with decreasing range of stem volume. The number of significant independent variables also decreases with decreasing range of stem volume (and decreasing number of observations). The last case with only 19 observations renders the whole regression insignificant at 5% significance level. Of the scenes acquired during growing season (S95Jul, S95Sep, and S95Oct), which are highly correlated among themselves, only one (S95Jul) has a significant contribution to the multivariate regression. The dry winter scene Dry93Feb, which alone does not correlate well with stem volume, is so uncorrelated with summer scenes that it adds a significant contribution to the multivariate regression in 3 cases out of 5.

In the second set of cases, the correlation coefficient first increases with decreasing range of stem volume. After reaching the saturation zone (somewhere around 50...150 m^3/ha), the correlation coefficient does no longer increase with decreasing range of stem volume (and decreasing number of observations). The number of significant independent variables again decreases with decreasing stem volume range (and decreasing number of observations). Again, the only summer acquisition with a significant contribution is the July scene (S95Jul). Even this scene becomes insignificant at 0–100 m^3/ha (with 95 observations). This is due to the high correlation between the summer scenes and the wet winter scene (Wet95Jan).

An attempt was made to derive an optimal 2-piece linear regression model for stem volume estimation (a) using all three summer scenes in an average summer scene, and (b) using the scenes as independent variables (see Table 4). Use of an average summer scene seems not to improve over the original bands. Computation of two models in image form showed that the 2-piece linear regression model with

Table 3
Multivariate regression results as a function of stem volume range

Vol-Rg	n	R^2	r	R_A^2	Dry93Feb	Wet95Jan	S95Jul	S95Sep	S95Oct	Dry98Mar
0–360	206	0.71	0.85	0.70	S	S	S	–	–	S
50–360	139	0.37	0.61	0.34	S	–	S	–	–	–
100–360	112	0.35	0.59	0.31	S	–	S	–	–	–
150–360	59	0.43	0.65	0.37	–	S	S	–	–	–
200–360	19	0.53	0.73	0.33	–	–	–	–	–	–
0–300	202	0.77	0.87	0.76	S	S	S	–	–	S
0–250	202	0.77	0.87	0.76	S	S	S	–	–	S
0–200	187	0.79	0.89	0.78	–	S	S	–	–	S
0–150	152	0.83	0.91	0.82	–	S	S	–	–	S
0–100	95	0.83	0.91	0.82	–	S	–	–	–	S
0–50	67	0.64	0.80	0.61	–	S	–	–	–	S

S = significant at 5% risk, – = not significant.

Table 4
Multivariate regression results with summer scenes averaged

Vol-Rg	n	R^2	r	Dry93Feb	Wet95Jan	S95Jul	Dry98Mar	Summer
0–360	206	0.70	0.82	–	S	0	S	S
0–100	95	0.83	0.91	–	S	0	S	–
0–150	152	0.82	0.91	–	S	0	S	S
100–360	112	0.24	0.49	–	–	0	–	S
150–360	59	0.38	0.62	–	S	0	–	S
0–150	152	0.82	0.91	0	S	0	S	S
0–150	152	0.83	0.91	0	S	S	S	0
150–360	59	0.36	0.60	0	S	0	0	S
150–360	59	0.40	0.63	0	S	S	0	0

S=significant at 5% risk level, –=not significant, 0=not included in the analysis.

original bands only (the last and third-last lines of Table 4) did not produce reliable stem volume estimates for the test site. In Table 4, column r gives the correlation coefficient between the estimated stem volume and ground data.

A 2-piece linear estimator was designed based on the regression experiments above. Since summer scenes are highly correlated, an average was computed over the 3 summer scenes (S95Jul, S95Sep, and S95Oct). The combined estimator used one winter-time wet-condition scene (scene Wet95Jan), one winter-time dry-condition scene (Dry98Mar), and the average summer scene. Two estimates were computed: e_L for lower volume range and e_H for upper volume range:

$$e_L = -118.8 + 0.243*W - 0.056*D \quad (10)$$

$$e_H = -174.9 + 0.183*W - 0.239*D + 0.273*S \quad (11)$$

where W=amplitude in the winter-wet scene, D=amplitude in the winter-dry scene, and S=amplitude in the summer average scene.

The decision which estimate to use was based on the SAR-derived estimates, not on ground data. This is essential for an estimator that must be applicable also outside study areas with ground data. If $e_H > 100$ m^3/ha, e_H was assigned as the combined estimate, e_L otherwise. The division point was determined by visual analysis of regression data. Within a zone of ±20 m^3/ha around the dividing line of 100 m^3/ha, the combined estimate was computed as a weighted average of e_L and e_H:

$$\begin{aligned} &\text{if } e_H > 120: && e = e_H \\ &\text{if } e_H < 80: && e = e_L \\ &\text{if } e_H \geq 80 \text{ and } e_H \leq 120: && e = ((120 - e_H)/40)e_L + ((e_L - 80)/40)e_H \end{aligned} \quad (12)$$

The application of the 2-piece linear regression model for mapping large forest areas is difficult because acquiring the needed winter-wet scene (and winter dry scene) depends on weather.

Fig. 4 shows the combined estimate against ground data in the stand-wise dataset. The RMSE was 28.5 m^3/ha. As most input SAR data are from the year 1995, the reference year of the estimate is 1995.

The combined estimate of stem volume was computed over the whole area where rectified JERS SAR data existed. To reduce the effects of speckle, JERS SAR scenes were filtered by the 5-out-of-9 filtering technique described earlier. The standard deviation of the Gaussian weight function was set to half a pixel (with 25-m pixel spacing).

Fig. 5 shows the combined estimate for a sub-window (4 km by 4 km) of the study site. The water mask was made with Landsat TM (near-infrared) data. An extract from an Ikonos multispectral (true colour) image is also shown for comparison. Recent clear-cut areas are fairly well presented in the stem volume estimate. Locations of high-estimate areas also correspond well with the locations of mature forests.

Fig. 6 shows the combined stem volume estimate over an area of 38 km by 38 km. The water mask was made with Landsat-TM data. The black triangle at the South-western corner is due to lack of coverage in one of the five JERS SAR scenes used.

The accuracy of the JERS-SAR-based stem volume estimate was tested using the point-wise dataset of stem volume measurements. The root-mean-square error between the JERS estimate and the ground measurement was 59.8 m^3/ha. The average stem volume in the ground dataset was

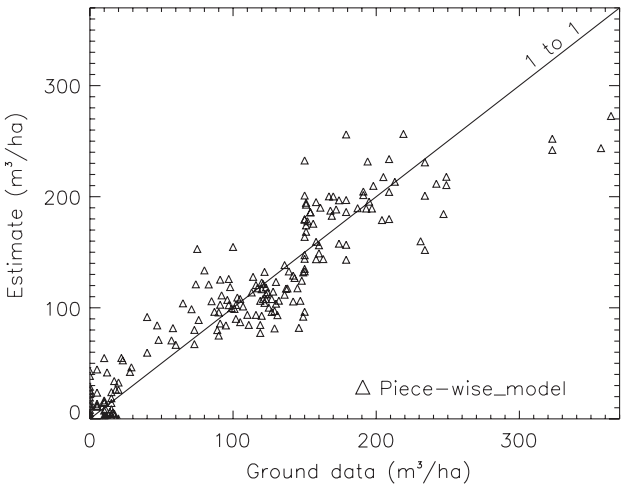

Fig. 4. Regression result: combined stem volume estimate vs. ground-measured stem volume.

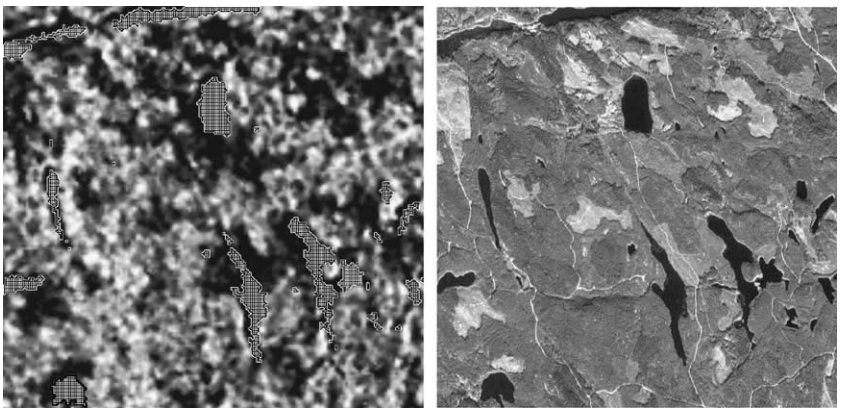

Fig. 5. Stem volume estimate using 5-date JERS SAR data (left) and Ikonos 4-m multispectral image. The scaling of stem volume shows the range 0...200 m^3/ha as black to white. Ikonos image: "Includes material (c) Space Imaging L.P."

104 m^3/ha and the maximum 355 m^3/ha. The average stem volume in the JERS-SAR-based stem volume estimate was 89 m^3/ha and the maximum 218 m^3/ha. The correlation coefficient between the estimated and measured stem volume was 0.57. The correlation in this point-wise dataset is lower than in the stand-wise dataset used as training data. This is partly due to speckle and other noise sources in the SAR data. Averaging SAR data over forest stands reduces speckle and enhances the relationship between forest biomass and SAR backscatter. Stand-wise averaging is a standard technique in studies of forest biomass and SAR. Another reason for the somewhat low accuracy is the difference in spatial scale between the datasets. The diameter of a ground measurement plot is of the order of 25 m. The JERS-based estimate was computed from a dataset where SAR pixels were averaged in a 75-m by 75-m window.

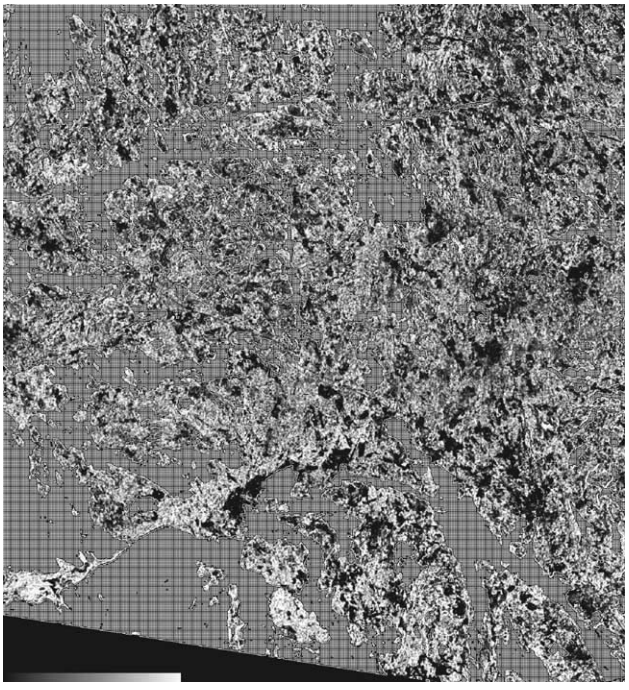

Fig. 6. JERS-based stem volume estimate over a 38-km-by-38-km area in Ruokolahti.

3.4. JERS-TM synergy

Regression analysis and stand-wise averaged JERS SAR and Landsat TM data were used to study the synergy between L-band SAR and optical data in forest biomass estimation. Landsat TM bands 2 (green visible light), 3 (red visible light), 4 (near-infrared), 5 (middle-infrared), and 7 (middle-infrared) were included in the analyses. Atmospheric corrections were applied to Landsat TM data and the pixel values were proportional to surface reflectance. Band 1 (blue visible light) of TM data was left out due to noise and band 6 (thermal band) due to lack of consistency from scene to scene in forest biomass estimation. NDVI (TM4 − TM3)/(TM4 + TM3) was also tested. Because NDVI had a low coefficient of determination (32%), it was left out in further analysis. Table 5 shows the correlation coefficient and coefficient of determination for a number of combinations of JERS acquisition dates and TM spectral bands. Column r in Table 5 gives the correlation coefficient between the estimated stem volume and ground data. The multi-temporal regression results shown on the first row of Table 3 is also shown here for convenience. The JERS regression was made in one unit over the whole range of stem volumes, not using the 2-piece approach defined by Eqs. (10)–(12). Multiple correlation coefficients of the order of 0.85 were obtained both for JERS data and TM data when these datasets were analysed

Table 5
Regression analysis of combined JERS SAR and Landsat TM data

Bands	r	R^2	n
JERS, 6 dates	0.85	0.71	206
TM, 5 bands	0.85	0.73	206
TM, bands 3 and 4	0.85	0.72	206
JERS + TM, all bands	0.89	0.79	206
JERS + TM, significant bands	0.88	0.77	206

separately. The corresponding coefficient of determination (R^2) was about 0.7, i.e., 70%. When combining optical (TM) and microwave (JERS) sensors, the correlation coefficient rose to almost 0.9 and the coefficient of determination to over 0.75 (75%). When restricting to only those bands in the JERS+TM combination that were significant at 5% significant level (TM band 3 and JERS scenes Dry93Feb and S95Jul), the correlation coefficient did not drop much.

Fig. 7 shows some of the regression results in graphical form. Triangles (top left) are Landsat TM estimates, squares (top right) JERS estimates, and diamonds (bottom left) JERS-TM estimates. One of the problems in Earth-observation-based forest biomass estimation is the saturation of the estimate at a fairly low level of biomass both for optical data and for L-band microwave data. Combination of sensors seems to alleviate this problem somewhat because the highest JERS-TM estimates are higher than either of the single-sensor estimate (the upper most dashed regression line at higher stem volumes in the bottom right figure belongs to the JERS-TM estimate). Similarly the lowest biomass estimates are slightly better in the JERS-TM estimate than in the single-sensors estimates. The slope of the regression line (slightly higher for the JERS-TM data) also reflects this phenomenon.

4. Conclusions

The single-date regression analysis showed that the stem volume vs. L-band backscatter relationship is very stable over the summer period. The regression models obtained in Ruokolahti site fit well with the model (for low biomass values) of Harrell et al. (1995). The fit between the Ruokolahti model and the model by Fransson and Israelsson (1999) was not as good, but the difference is within the limits of calibration accuracy of the JERS SAR sensor. The stability of the regression models from scene to scene suggests that a constant regression model could be used in mapping boreal forest biomass using a single summer acquisition. This could be applied, e.g., to wide area mosaics produced in the GBFM project (Rosenqvist et al., 2000) if accuracy requirements are low and if biomass is aggregated to larger units before the data are used in quantitative models. Eqs. (5) and (6) above could be used for stem volume and biomass when the available Earth observation data are from an L-band SAR (HH-polarized, nominal incidence angle 39°) and the scenes have been acquired in summer conditions. This type of wide area biomass estimation would ideally require well-calibrated L-band SAR data. For instance, an increase of 1.86 dB due to calibration error increases the stem volume estimate from

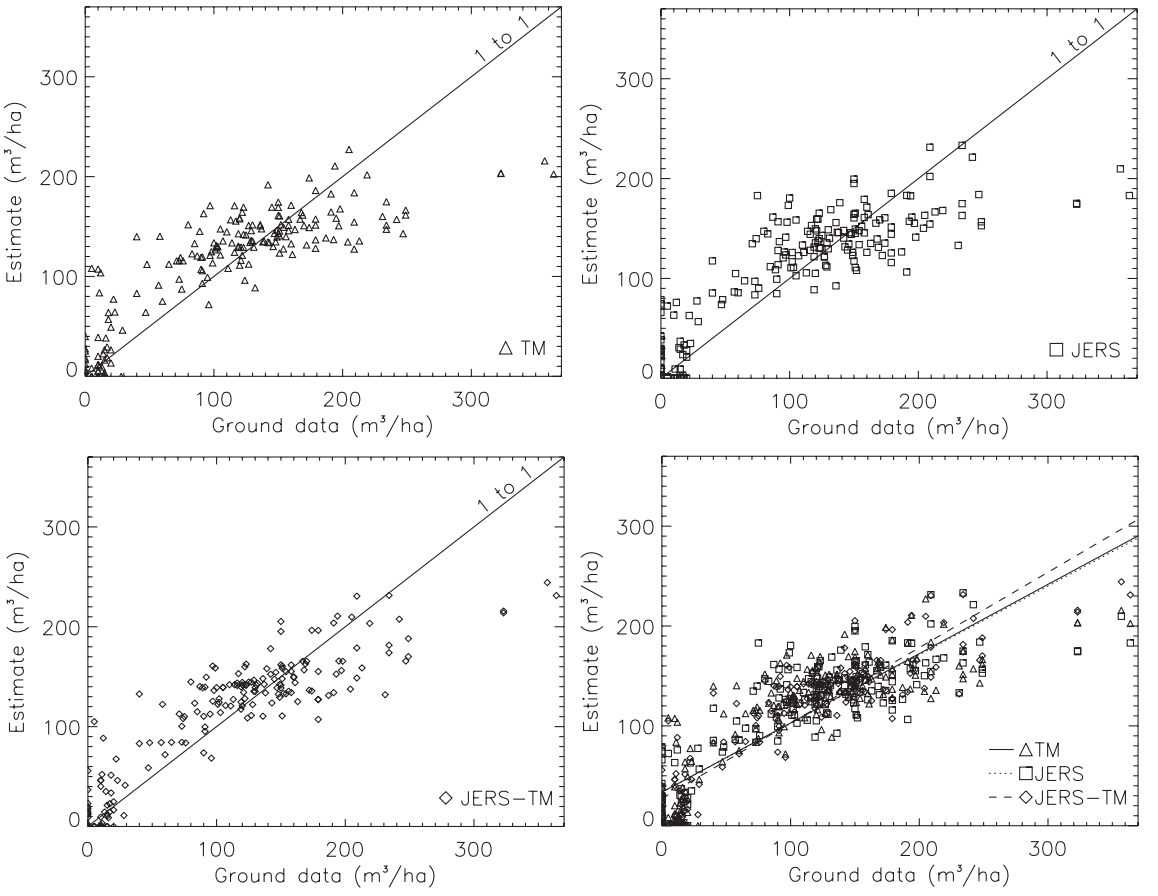

Fig. 7. Estimated vs. ground-observed stem volume for Landsat TM data (top left), JERS data (top right), both datasets combined (bottom left). The last sub-figure (bottom right) shows all three estimates with their linear regression lines in the same diagram.

100 m^3/ha to 275 m^3/ha. A calibration accuracy of 0.7 dB produces an increase from 100 m^3/ha to 162 m^3/ha, which is better in balance with the estimation accuracy (60 m^3/ha).

The high correlation ($r=0.85$) obtained in regression modelling between multi-temporal JERS SAR data and forest stem volume data suggests that multi-temporal L-band SAR data can be used for forest biomass mapping for large stands and forest management units larger than stands. Data from varying winter conditions, in addition to summer data, were used to obtain the correlation coefficient of 0.85. In winter data, the relationship between L-band backscatter and forest biomass varies widely from scene to scene. The regression model is applicable in scenes acquired in the same meteorological conditions as those used to derive the regression model. In practice, this technique requires reference data within each mapped scene. This technique can be efficient for areas that consist of one or a few scenes (along an orbit). For larger areas, e.g., for continental mapping, multi-temporal image acquisitions in uniform meteorological conditions are practically impossible. Even in a local context, the mapping of high-biomass areas (e.g., dry biomass greater than 100 tons/ha) is not accurate.

The use of optical Landsat TM data, in addition to JERS SAR data, improved the biomass estimation accuracy slightly (r increased from 0.85 to 0.89). The inclusion of optical data also improved the saturation of the regression model. Since the only significant optical bands in the SAR-optical regression model were the red and near-infrared bands, data from practically all optical satellites can be used.

A detailed (25-m pixel spacing, 2-m vertical accuracy) DEM was used when analysing the JERS SAR data of the Ruokolahti study site. For wide-area biomass mapping, the acquisition of a DEM of the same standard is costly if such a DEM is available at all. Global DEM data are too coarse for radiometric normalization of topographic effects in JERS SAR data. An accurate and detailed DEM is essential for pixel-wise biomass estimation because even a 5° slope (towards the sensor) causes a change of 63 m^3/ha in the stem volume estimate. If biomass mapping is made for larger areal units, the topographic effects can be expected to cancel out from the averaged biomass estimate if the estimation unit includes equal areas of fore-slopes and back-slopes.

Acknowledgements

The work described in this paper was funded by TEKES in the context of “MODIS biomass” project. JERS SAR data were supplied by NASDA (currently JAXA) in the context of the GBFM North Europe science node. Stora Enso Ltd. supplied the stand-wise forest inventory data. Finnish Forest Research Institute supplied the point-wise ground data. Dr. Ranga B. Myneni (the principal investigator of NASA project NAS 13-98048) is acknowledged for supplying the Ikonos scene of a part of the study site. The author also wants to thank Mrs. Eija Parmes of VTT for re-formatting and processing the forest inventory data, Mrs. Brita Veikkanen of VTT for geo-coding Landsat TM data, and Dr. Hans Jonsson of Metria Miljoanalys for his assistance in ordering JERS SAR data. Dr. Tuomas Häme of VTT provided valuable comments to improve the clarity of the manuscript.

References

Beaudoin, A., Le Toan, T., Goze, S., Hsu, C., Han, H., Kong, J., et al. (1992). Retrieval of forest biomass from SAR data. *Proceedings of the Final Workshop of the MAESTRO/AGRISCATT Campaigns, Noordwijk, 6–7 March 1992* (pp. 123–130).

Chipman, J., Lillesand, T., Gage, J., & Radcliffe, S. (2000). Spaceborne imaging radar in support of forest resource management. *Photogrammetric Engineering and Remote Sensing*, *66*(11), 1357–1366.

De Grandi, G., Mayaux, P., Rauste, Y., Rosenqvist, Å., Simard, M., & Saatchi, S. (2000). The global rain forest mapping project JERS-1 radar mosaic of tropical Africa: Development and product characterisation aspects. *IEEE Transactions on Geoscience and Remote Sensing*, *38*(5), 2218–2233.

Dobson, C., Mc Donald, K., Ulaby, F., & Sharik, T. (1991). Relating the temporal change observed by AIRSAR to surface and canopy properties of mixed conifer and hardwood forests of Northern Michigan. *Proceedings of the Third Airborne Synthetic Aperture Radar (AIRSAR) Workshop, May 23–24, 1991. JPL Publication*, *vol. 91–30* (pp. 34–43).

Dobson, C., Ulaby, F., Pierce, L., Sharik, T., Bergen, K., Kellndorfer, J., et al. (1995). Estimation of forest biophysical characteristics in Northern Michigan with SIR-C/X-SAR. *IEEE Transactions on Geoscience and Remote Sensing*, *33*(4), 877–894.

Dobson, C. K., Ulaby, F., Le Toan, T., Beaudoin, A., Kasischke, E., & Christensen, N. (1992). Dependence of radar backscatter on coniferous forest biomass. *IEEE Transactions on Geoscience and Remote Sensing*, *30*(2), 412–415.

Fransson, J., & Israelsson, H. (1999). Estimation of stem volume in boreal forests using ERS-1 C- and JERS-1 L-band SAR data. *International Journal of Remote Sensing*, *20*(1), 123–137.

Fransson, J., Smith, G., Askne, J., & Olsson, H. (2001). Stem volume estimation in boreal forests using ERS-1/2 coherence and Spot XS optical data. *International Journal of Remote Sensing*, *22*(14), 2777–2791.

Green, R. (1998). Relationship between polarimetric SAR backscatter and forest canopy and sub-canopy biophysical properties. *International Journal of Remote Sensing*, *19*(12), 2395–2412.

Häme, T., Salli, A., & Lahti, K. (1992). Estimation of carbon storage in boreal forest using remote sensing data, Pilot study. In M. Kanninen, & P. Anttila (Eds.), The Finnish programme on climate change, Progress report. *Publications of the Academy of Finland*, *vol. 3/92* (pp. 250–255). Helsinki, Finland: VAPK Publishing.

Harrell, P., Bourgeau-Chavez, L., Kasischke, E., French, N., & Christensen, N. (1995). Sensitivity of ERS-1 and JERS-1 radar data to biomass and stand structure in Alaskan boreal forest. *Remote Sensing of Environment*, *54*, 247–260.

Harrell, P., Kasischke, E., Bourgeau-Chavez, L., Haney, E., & Christensen, N. (1997). Evaluation of approaches to estimating aboveground biomass in Southern pine forests using SIR-C data. *Remote Sensing of Environment*, *59*, 223–233.

Imhoff, M. (1993). Radar backscatter/biomass saturation: Observations and implications for global biomass assessment. *Proceedings of IGARSS'93, 18–21 August 1993, Tokyo, Japan*, *vol. I* (pp. 43–45).

Imhoff, M. (1995). Radar backscatter and biomass saturation: Ramifications for global biomass inventory. *IEEE Transactions on Geoscience and Remote Sensing*, *33*(2), 511–518.

Israelsson, H., Askne, J., Fransson, J., & Sylvander, R. (1995). *JERS-1 SAR analysis of boreal forest biomass, Final report of JERS-1/ERS-1 system verification program, MITI and NASDA, March 1995, vol. II, p. 2–38...2–45.*

Israelsson, H., Askne, J., & Sylvander, R. (1992). Estimation of forest characteristics using multi frequency polarimetric SAR data. *Proceedings of the Final Workshop of the MAESTRO/AGRISCATT Campaigns, Noordwijk, 6–7 March 1992* (pp. 47–51).

Israelsson, H., Ulander, L., Askne, J., Fransson, J., Frölind, P., Gustavsson, A., et al. (1997). Retrieval of forest stem volume using VHF SAR. *IEEE Transactions on Geoscience and Remote Sensing*, *35*(1), 36–40.

Jonsson, H. (2002). GBFM/Northern Europe science node initiation. *Proceedings of the 1st Science Meeting—GBFM/NE, Stockholm, Sweden, 7–8 February 2002*. Metria Miljöanalys. 16 p.

Kasischke, E., Bourgeau-Chavez, L., Christensen, N., & Dobson, C. (1991). The relationship between aboveground biomass and radar backscatter as observed on airborne SAR imagery. *Proceedings of the Third Airborne Synthetic Aperture Radar (AIRSAR) Workshop, May 23–24, 1991. JPL Publication*, *vol. 91–30* (pp. 11–21).

Kasischke, E., Bourgeau-Chavez, L., Christensen, N., & Haney, E. (1994). Observations on the sensitivity of ERS-1 SAR image intensity to changes in aboveground biomass in young loblolly pine forests. *International Journal of Remote Sensing*, *15*(1), 3–16.

Kasischke, E., Christensen, N., & Bourgeau-Chavez, L. (1995). Correlating radar backscatter with components of biomass in Loblolly pine forests. *IEEE Transactions on Geoscience and Remote Sensing*, *33*(3), 643–659.

Kellndorfer, J., Dobson, C., & Pierce, L. (2001). Forest biometrics from ERS and JERS in Michigan. *Proceedings of IGARSS'2001* (pp. 780–782).

Kuplich, T., Salvatori, V., & Curran, P. (2000). JERS-1/SAR backscatter and its relationship with biomass of regenerating forests. *International Journal of Remote Sensing*, *21*(12), 2513–2518.

Kurvonen, L., Pulliainen, J., & Hallikainen, M. (1999). Retrieval of biomass in boreal forest from multitemporal ERS-1 and JERS-1 SAR images. *IEEE Transactions on Geoscience and Remote Sensing*, *37*(1), 198–205.

Le Toan, T., Beaudoin, A., & Guyon, D. (1992). Relating forest biomass to SAR data. *IEEE Transactions on Geoscience and Remote Sensing*, *30*(2), 403–411.

Le Toan, T., Beaudoin, A., Riom, J., & Guyon, D. (1991). Relating forest biomass to SAR data. *Proceedings of the International Geoscience and Remote Sensing Symposium IGARSS'91, Helsinki University of Technology, Espoo, Finland, June 3–6, 1991*, *vol. II* (pp. 689–692).

Luckman, A., Baker, J., Honzak, M., & Lucas, R. (1998). Tropical forest biomass density estimation using JERS-1 SAR: Seasonal variation, confidence limits, and application to image mosaics. *Remote Sensing of Environment*, *63*, 126–139.

Luckman, A., Baker, J., Kuplich, T., Yanasse, C., & Frery, A. (1997). A study of the relationship between radar backscatter and regenerating tropical forest biomass for spaceborne SAR instruments. *Remote Sensing of Environment*, *60*, 1–13.

Luckman, A., Baker, J., & Wegmüller, U. (2000). Repeat-pass interferometric coherence measurements of disturbed tropical forest from JERS and ERS satellites. *Remote Sensing of Environment*, *73*, 350–360.

Melon, P., Martinez, J., Le Toan, T., Ulander, L., & Beaudoin, A. (2001). On the retrieving of forest stem volume from VHF SAR data: Observation and modeling. *IEEE Transactions on Geoscience and Remote Sensing*, *39*(11), 2364–2372.

Moghaddam, M., Durden, S., & Zebker, H. (1994). Radar measurement of forested areas during OTTER. *Remote Sensing of Environment*, *47*, 154–166.

Paloscia, S., Macelloni, G., Pampaloni, P., & Sigismondi, S. (1999). The potential of C-band and L-band SAR in estimating vegetation biomass: The ERS-1 and JERS-1 experiments. *IEEE Transactions on Geoscience and Remote Sensing*, *37*(4), 2107–2110.

Pulliainen, J., Engdahl, M., & Hallikainen, M. (2003). Feasibility of multi-temporal interferometric SAR data for stand-level estimation of boreal forest stem volume. *Remote Sensing of Environment*, *85*, 397–409.

Pulliainen, J., Heiska, K., Hyyppä, J., & Hallikainen, M. (1994). Backscattering properties of boreal forests at the C- and X-bands. *IEEE Transactions on Geoscience and Remote Sensing*, *34*(5), 1041–1050.

Pulliainen, J., Kurvonen, L., & Hallikainen, M. (1997). Effect of temporally varying parameters on L- and C-band SAR observations of boreal forests. *Proceedings of IGARSS'97, 3–8 August 1997, Singapore*, *vol. IV* (pp. 1874–1877).

Pulliainen, J., Kurvonen, L., & Hallikainen, M. (1999). Multitemporal behaviour of L- and C-band SAR observations of boreal forests. *IEEE Transactions on Geoscience and Remote Sensing*, *37*(2), 927–937.

Pulliainen, J., Mikkelä, P., Hallikainen, M., & Ikonen, J. (1996). Seasonal dynamics of C-band backscatter of boreal forests with applications to biomass soil moisture estimation. *IEEE Transactions on Geoscience and Remote Sensing*, *34*(3), 758–770.

Ranson, K., & Sun, Q. (1997). An evaluation of AIRSAR and SIR-C/X-SAR images for mapping northern forest attributes in Maine, USA. *Remote Sensing of Environment*, *59*, 203–222.

Rauste, Y. (1993). Multitemporal analysis of forest biomass using AIRSAR data. *Proceedings of the 25th International Symposium on Remote Sensing and Global Environmental Change, Graz, Austria, 4–8 April 1993*, *vol. I* (pp. 328–338).

Rauste, Y., Häme, T., Pulliainen, J., Heiska, K., & Hallikainen, M. (1994). Radar-based forest bio-mass estimation. *International Journal of Remote Sensing*, *15*, 2797–2808.

Rauste, Y., Heiska, K., & Pulliainen, J. (1992). On forest inventory and elevation determination using polarimetric radar data. *Proceedings of the Final Workshop of the MAESTRO/AGRISCATT Campaigns, Noordwijk, 6–7 March 1992* (pp. 117–121).

Rignot, E., Zimmermann, R., & van Zyl, J. (1995). Spaceborne applications of P band imaging radars for measuring forest biomass. *IEEE Transactions on Geoscience and Remote Sensing*, *33*(5), 1162–1169.

Rosenqvist, Å. (1996). Evaluation of JERS-1, ERS-1 and Almaz SAR backscatter for rubber and oil palm stands in West Malaysia. *International Journal of Remote Sensing*, *17*, 3219–3231.

Rosenqvist, Å., Shimada, M., Chapman, B., Freeman, A., De Grandi, G., Saatchi, S., et al. (2000). The global rain forest mapping project—a review. *International Journal of Remote Sensing*, *21*(6–7), 1375–1387.

Shimada, M. (1996). Radiometric and geometric calibration of JERS-1 SAR. *Advances in Space Research*, *17*(1), 79–88.

Shimada, M. (2001). *User's guide to NASDA's SAR products Ver.2*. Tokyo, Japan: NASDA 2001 (Aug. 9) 23 pp.

Shimada, M., & Isoguchi, O. (2002). JERS-1 SAR mosaics of Southeast Asia using calibrated path images. *International Journal of Remote Sensing*, *23*(7), 1507–1526.

Skriver, H., & Gudmandsen, P. (1992). Analysis of MAESTRO-1 polarimetric SAR data of forest areas at Les Landes. *Proceedings of the Final Workshop of the MAESTRO/AGRISCATT Campaigns, Noordwijk, 6–7 March 1992* (pp. 131–136).

Smith, G., Dammert, P., Santoro, M., Fransson, J., Wegmuller, U., & Askne, J. (1998). Biomass retrieval in boreal forest using ERS and JERS SAR. *Proceedings of the Retrieval of Bio- and Geo-Physical Paramaters from SAR Data for Land Applications Workshop*. Noordvijk, The Netherlands: ESA/ESTEC.

Toshio, S., Takuhiro, N., Takuro, Y., Keiji, O., Sotaro, T., & Toshiro, S. (1995). *Applicability of JERS-1 SAR data for monitoring of forest function and environment: Analysis of forest stand structure using JERS-1 SAR data for forest management, Final report of JERS-1/ERS-1 system verification program, MITI and NASDA, March 1995, vol. II, p. 2–38...2–45.*

Wang, Y., Kasischke, E., Melack, J., Davis, F., & Christensen, N. (1994). The effects of changes in loblolly pine biomass and soil moisture on ERS-1 SAR backscatter. *Remote Sensing of Environment*, *49*, 25–31.